

Mass and low-lying levels of $^{106,108}\text{In}$ from the $^{106,108}\text{Cd}(p,n\gamma)$ reactions

B. W. Filippone,* C. N. Davids, and R. C. Pardo
Argonne National Laboratory, Argonne, Illinois 60439

J. Äystö

University of Jyväskylä, Jyväskylä, Finland

(Received 19 December 1983)

^{106}In has been studied via the reaction $^{106}\text{Cd}(p,n\gamma)^{106}\text{In}$ in the energy range $E_p=7-9$ MeV. In-beam γ -ray excitation functions, γ - γ coincidence measurements, and β^+ -delayed γ -ray excitation functions have been used to identify thirteen levels in ^{106}In . From this new level scheme the energy separation of the high-spin ground state and the low-spin isomer has been determined to be 28.6 ± 0.5 keV. The threshold energy of the strongest low-lying γ -ray transition yields a mass excess for ^{106}In of -80601 ± 15 keV. Spins for some states are suggested by comparing the excitation functions to Hauser-Feshbach calculations. In-beam γ -ray excitation functions for the $^{108}\text{Cd}(p,n\gamma)^{108}\text{In}$ reaction give a mass excess for the 3^+ β^+ -decaying state in ^{108}In of -84018 ± 12 keV. The systematics of odd-odd In nuclei are discussed in a j - j coupling model.

I. INTRODUCTION

Studies of the systematics of the masses of very neutron-deficient nuclei near $Z=50$ rely on the masses of a number of nuclides close to stability,¹ including such nuclei as $^{106,108}\text{In}$. In addition, the study of the low-lying level structure of odd-odd nuclei provides information on the residual neutron-proton interaction. However, possibly because of the complexity brought on by the coupling of this extra neutron and proton, data on odd-odd nuclei near $A\approx 100$ are extremely sparse. In particular, for the even- A In nuclei with $A < 112$, one finds that in a simple shell-model picture, a $1g_{7/2}$ proton hole is coupled to a $1g_{7/2}$ or $2d_{5/2}$ neutron quasiparticle. This results in a large number of states with widely differing spins, each split by the residual interaction. In this instance, two low-lying β^+ -decaying states appear, one having high spin and the other having low spin. Their relative location is not well determined in most cases.

The tabulated value of the mass excess of ^{106}In , -80586 ± 31 keV,² is based on a single measurement of the positron end point by Catura and Richardson.³ The mass excess for the low-spin β^+ -decaying state in ^{108}In is given as -84100 ± 80 keV,² also from a positron end point measurement.

Previous information on the low-lying levels in ^{106}In has been obtained from β^+ -decay studies of ^{106}Sn .^{1,4,5} In addition, studies of the β^+ decay of ^{106}In (Refs. 3 and 6-10) have confirmed the existence of two β^+ -decaying states, one of high spin and one of spin $J=3$. Recent low-temperature nuclear orientation experiments¹¹ have established $J=7$ for the high-spin β^+ -decaying state.

The work described here was initiated to measure the mass of ^{106}In via the $^{106}\text{Cd}(p,n\gamma)^{106}\text{In}$ threshold. A preliminary measurement of γ -ray excitation functions revealed some disagreements with the location of the lowest-lying states given by Varley *et al.*⁵ In order to extract a reliable mass excess from excited-state thresholds,

a knowledge of the level scheme is necessary. Therefore a detailed study of the low-lying states in ^{106}In was undertaken. Using excitation functions for prompt and beta-delayed γ rays from the $^{106}\text{Cd}(p,n\gamma)^{106}\text{In}\rightarrow^{106}\text{Cd}$ reaction, along with γ - γ coincidence data, a new level scheme for ^{106}In has been deduced. A reordering of the two lowest states seen by Varley *et al.*⁵ and six new levels have been found. From the deduced level scheme the energy separation of the high-spin (6.3 min) and low-spin (5.3 min) states is 28.6 keV, with the high-spin state being the ground state. Hauser-Feshbach calculations have been used to suggest spins for some of the low-lying levels from the relative γ -ray excitation functions. With this information the systematics of the low-lying states of odd-odd In isotopes are discussed in terms of a j - j coupling model.

The same technique of extracting the mass excess from γ -ray thresholds in the $(p,n\gamma)$ reaction has also been used to determine the mass excess of the 3^+ beta-decaying state in ^{108}In . Because the γ -ray excitation functions from the present work were consistent with the level scheme proposed by Hseuh and Macias¹² [using ^{108}Sn decay and in-beam γ rays from $^{108}\text{Cd}(p,n\gamma)^{108}\text{In}$], a detailed study of low-lying states in ^{108}In was not carried out.

II. EXPERIMENTAL PROCEDURE

For the ^{106}In experiment, a 90% enriched 6.3 mg/cm² ^{106}Cd target was bombarded with protons from the Argonne National Laboratory FN tandem accelerator. Beam currents were typically 10-30 nA except for the γ - γ coincidence experiment where only 1-2 nA was needed because of the much closer geometry used. For the low-energy excitation functions and the mass measurements, the entrance and exit slits of the analyzing magnet were set at 0.89 mm to precisely define the beam trajectory. The resulting energy resolution was about ± 5 keV. This was important in ensuring reproducibility of energies and for providing precise energy steps. Calibration of the

magnet was done using the known laboratory threshold of 7318 keV for the 226-KeV γ ray from the $^{60}\text{Ni}(p,n\gamma)^{60}\text{Cu}$ reaction. The excited state in ^{106}In used for the mass measurement has a laboratory threshold of approximately 7.5 MeV.

The beam energy was changed in steps of 10 or 15 keV between 7.4 and 8.4 MeV for the in-beam excitation functions and in steps of 25 keV from 7.3 to 7.9 MeV for the β^+ -delayed γ -ray excitation functions. The coincidence experiment was performed at 8.9 MeV.

For the in-beam experiments a 10% relative efficiency Ge(Li) detector and a 100 mm² by 10 mm intrinsic Ge detector were used to observe γ rays. Thin Fe sheets were inserted between the target and detectors to absorb low-energy target x-rays. The detectors were placed at $\pm 90^\circ$ for the early threshold experiments, and later at $+55^\circ$ and -125° to minimize angular distribution effects for the comparison of excitation functions in the statistical model calculations. All detectors were calibrated and efficiencies measured using standard calibrated sources.

Gamma-ray yields, extracted off line, were normalized to total charge collected on the Faraday cup and corrected for data-acquisition dead time. This correction was made either by gating the current integrator with the computer busy signal, or by sending a pulser signal through the detector preamplifier.

For the decay experiment a shielded 15% relative efficiency Ge(Li) detector was used in conjunction with a single-rabbit transfer system. The target was bombarded for 30 sec and then transferred to the Ge(Li) detector and counted during a beam-off period for 512 sec, with the timing determined by a crystal-controlled sequence timer. The times were chosen to minimize buildup of activities while maximizing statistical accuracy. The data were corrected for the time dependence of both the beam and the detector dead time by generating a time spectrum for each with a multiscaling analog-to-digital converter (ADC). In addition, the γ -ray yields were corrected for the buildup of activity from the previous bombardments.

A 58% enriched ^{108}Cd metal target was used for the $^{108}\text{Cd}(p,n\gamma)^{108}\text{In}$ experiment. The detectors and detector geometry (with detectors at $\pm 90^\circ$) were the same as for the ^{106}In in-beam excitation function measurements. Energy steps of 10 keV were used for $E_p = 5.9$ –6.5 MeV. The analysis of the data was as described above.

III. RESULTS

A. ^{106}In level scheme

Gamma rays were identified as being associated with ^{106}In by means of γ -ray thresholds and/or coincidence relationships with known transitions. All γ rays seen by previous workers in the decay of ^{106}Sn were seen in the present experiment. In addition, many new γ rays were seen to have a threshold near the mass of ^{106}In or were found to be in coincidence with known γ rays in ^{106}In . Gamma-ray spectra from the $^{106}\text{Cd}(p,n\gamma)^{106}\text{In}$ reaction at $E_p = 9.0$ MeV are shown in Fig. 1. Table I lists the γ rays assigned to ^{106}In .

The γ - γ coincidence experiment revealed that the

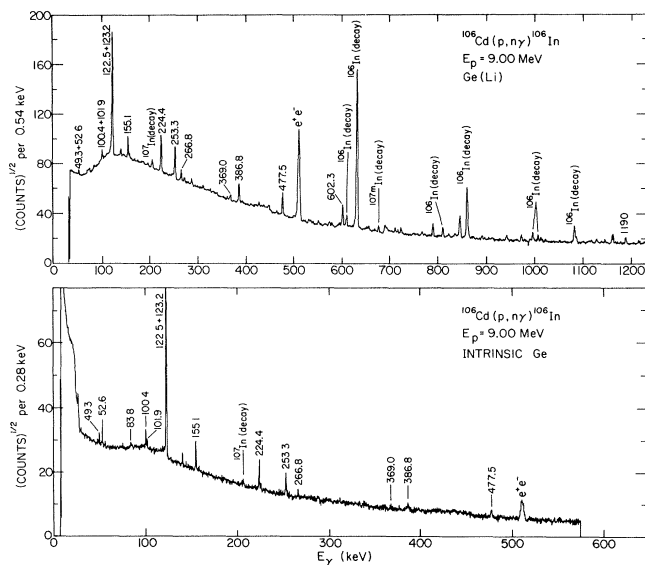


FIG. 1. In-beam γ -ray spectra from the $^{106}\text{Cd}(p,n\gamma)^{106}\text{In}$ at $E_p = 9.00$ MeV obtained with a Ge(Li) and an intrinsic Ge detector.

122.6-keV γ ray seen in the singles experiment was actually a doublet composed of a strong 122.5-keV γ ray and a weak 123.2-keV γ ray. By setting gates on the individual channels of the 122.6-keV peak in one detector and extracting the yield of coincident γ rays in the other detector as a function of channel number, two families of γ rays were revealed to be in coincidence with one or the other member of the doublet. Examples of such yield curves are given in Fig. 2. The difference between the centroids of these curves gives an energy separation of the two γ rays of 0.65 ± 0.10 keV. All the coincidence data are summarized in the coincidence matrix shown in Table II. Backgrounds were subtracted from the coincidence spectra by setting gates on regions adjacent to the peaks.

The γ -ray excitation thresholds were determined by fitting the γ -ray yield taken to the two-thirds power to a straight line versus proton energy. This method assumes $l=0$ neutrons in the final state and an infinite target thickness. The assumption of $l=0$ neutrons will be discussed in Sec. III D. Since the target was ~ 200 keV thick to 7.5-MeV protons, fitting the excitation functions for proton energies only up to 200 keV above the γ ray threshold validates the thick target assumption. Figure 3 shows the excitation functions for the 122.5-, 100.4-, and

TABLE I. ^{106}In γ rays seen in $^{106}\text{Cd}(p,n\gamma)^{106}\text{In}$ (energies in keV).

49.3 ± 0.1	224.4 ± 0.2	477.5 ± 0.3
52.6 ± 0.1	247 ± 1	535 ± 1
83.8 ± 0.2	253.3 ± 0.2	602.3 ± 0.3
100.4 ± 0.1	266.8 ± 0.3	712 ± 1
101.9 ± 0.1	326 ± 1	725 ± 1
122.5 ± 0.1	369.0 ± 0.3	864 ± 1
123.2 ± 0.1	386.8 ± 0.3	1190 ± 0.5
155.1 ± 0.1	447 ± 1	

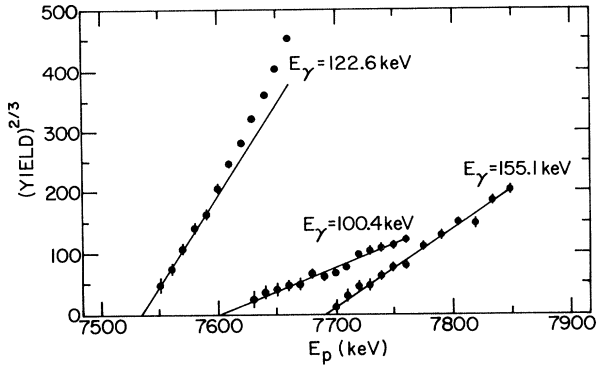


FIG. 3. Gamma-ray excitation functions for the 122.6-, 100.4-, and 155.1-keV γ rays. The yields have been corrected for detector efficiency and internal conversion.

ment with the ^{106}Sn decay experiments of Varley *et al.*⁵ and Plochocki *et al.*¹ However, the ordering of the 253-, 204-, and 151-keV levels disagrees with the ordering of Varley *et al.*⁵ Apparently the placements of Varley *et al.*⁵ were determined chiefly from coincidence relations which are in agreement with the present work, but the additional information from the γ -ray thresholds allows definitive placement of the low-lying states.

The level scheme of Fig. 4 shows the ground state of ^{106}In to be the high-spin beta-decaying state with the low-spin isomer located at an excitation energy of 28.6 keV. This is in contradiction with a previous β^+ end point

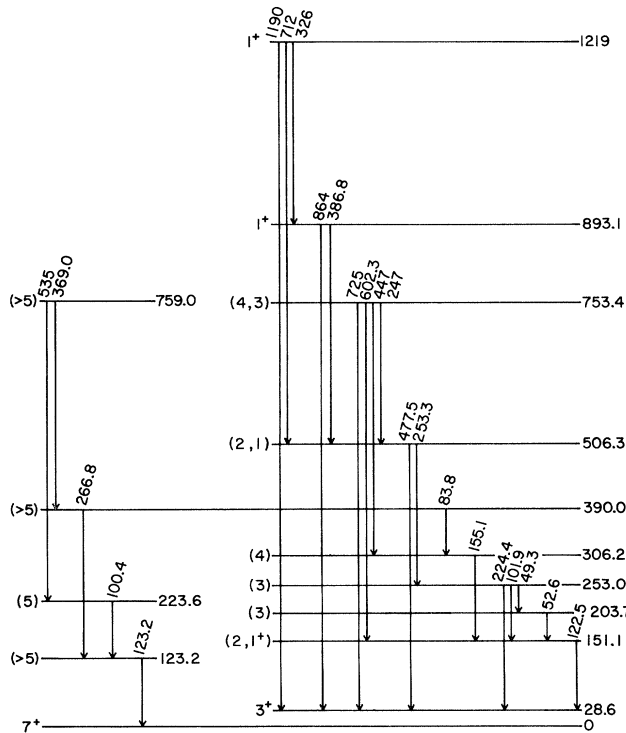


FIG. 4. ^{106}In level scheme inferred from the present work. Spins are those suggested from the statistical model calculations discussed in the text.

TABLE III. γ -ray thresholds relative to that of the 122.5-keV γ ray. $\Delta E_{\text{exp}} = E_{\text{thresh}}(E_\gamma) - E_{\text{thresh}}(122.5)$, $\Delta E_{\text{calc}} =$ calculated from level scheme of Fig. 4.

E_γ (keV)	ΔE_{exp} (keV)	ΔE_{calc} (keV)
49.3	82 ± 21	101.9
52.6	46 ± 11	52.6
100.4	68 ± 9	72.5
101.9	57 ± 40	101.9
155.1	156 ± 8	155.1
224.4	100 ± 10	101.9
253.3	346 ± 10	355
369.0	570 ± 50	608
386.8	721 ± 17	742
477.5	337 ± 13	355
602.3	595 ± 25	602

measurement,⁹ which indicated that the high-spin state appeared to be 400 ± 200 keV below the isomer. Because of this discrepancy, excitation functions were also measured for several ^{106}In beta-delayed γ rays using a rabbit transfer system. This technique allows a determination of thresholds for states which decay only by β^+ emission. The center-of-mass thresholds of the 633-, 861- (seen in the decay of both the high- and low-spin β^+ decaying states⁸ of ^{106}In), and 1716-keV (seen only in the low spin state decay^{8,9}) γ rays in ^{106}Cd were the same, and were located at 128 ± 15 keV below the threshold of the 122.5-keV γ ray. This is in agreement with the level scheme of Fig. 4 for direct population of the low spin β^+ decaying state by the $^{106}\text{Cd}(p,n)^{106}\text{In}(28.6)$ reaction. The 998- and 1009-keV γ rays in ^{106}Cd (seen only in the high spin decay^{8,9}) were found to have a threshold 44 ± 25 keV above the threshold of the 122.5-keV γ ray. This implies the virtual absence of direct population of the high-spin ground state, a possible weak population of the 123.2-keV state (located 28 keV below the 122.5-keV γ ray threshold), and a stronger feeding of the 223.6-keV state (located 72 keV above the 122.5-keV γ ray threshold) which promptly γ decays to the ground state. Because of the weak population of these states and the larger energy steps used for this experiment, a change in slope of the excitation function expected for direct excitation of states above the 223.6-keV state threshold could not be discerned.

B. Mass of ^{106}In

The measured laboratory threshold of the 122.5-keV γ ray was 7535 ± 10 keV, where the error is only statistical. This γ ray was chosen to determine the mass because it had the steepest excitation function and also the lowest threshold of the in-beam γ rays. The thresholds of the other γ rays were then used to determine level placement.

With the measured threshold of the 122.5-keV γ ray and the level scheme of Fig. 4, a mass excess of -80601 ± 15 keV is deduced for the ground state of ^{106}In . The uncertainty here includes beam energy spread and resonance effects of the type discussed by Freeman,¹³ as well as small deviations from a linear dependence of $(\text{yield})^{2/3}$ vs E_p which are discussed in Sec. III D. The ef-

TABLE IV. Comparison of measured ^{106}In mass excess with predictions.

Source	ΔM (MeV)	$\Delta M_{\text{calc}} - \Delta M_{\text{exp}}^k$ (MeV)
Meyers ^a	-81.37	-0.77
GHT ^b	-80.24	0.36
SH ^c	-81.8	-1.2
LZ ^d	-80.53	0.07
JGK ^e	-80.85	-0.25
CK ^f	-80.72	-0.12
JE ^g	-80.55	0.05
MS ^h	-80.85	-0.25
MN ⁱ	-80.47	0.13
Measurements		
This work	-80.601 \pm 0.015	
CR ^j	-80.615 \pm 0.031	

^aW. D. Meyers, At. Data Nucl. Data Tables **17**, 411 (1976), 1975 mass excess predictions, edited by S. Maripuu.

^bH. V. Groote, E. R. Hilf, and K. Takahashi, see footnote (a).

^cP. A. Seeger and W. M. Howard, see footnote (a).

^dS. Liran and N. Zeldes, see footnote (a).

^eJ. Jänecke, see footnote (a).

^fE. Comay and I. Kelson, see footnote (a).

^gJ. Jänecke and B. P. Eynon, see footnote (a).

^hJ. E. Monahan and F. J. D. Serduke, Phys. Rev. C **17**, 1196 (1978).

ⁱP. Möller and J. R. Nix, At. Data Nucl. Data Tables **26**, 165 (1981).

^jR. C. Catura and J. R. Richardson, Ref. 3 combined with the level scheme of Fig. 4.

^kPresent value for ^{106}In mass excess.

fect of the presence of the 123.2-keV γ ray was found to be negligible since this state is only weakly populated, as determined from the decay γ -ray excitation functions.

The mass excess given here is in good agreement with the value of -80.615 ± 30 keV deduced from the high-energy positron end point measurement of the $J=3^+$ state decay by Catura and Richardson³ when coupled with the level scheme of Fig. 4. A comparison of the measured mass excess with some recent theoretical predictions is shown in Table IV.

C. Multipolarities of states in ^{106}In

As mentioned previously in connection with Fig. 3, the change in slope of 122.5-keV γ -ray excitation function at about 50 keV above its threshold is attributed to additional feeding from the 203.7-keV state. By assuming $l=0$ neutrons in the final state and by comparing this increase in intensity with the measured intensity of the 52.6-keV γ ray, limits can be set on the internal conversion coefficient of the 52.6-keV γ ray and hence its multipolarity. This is done by balancing the intensity into and out of the 203.7-keV state. From the level scheme of Fig. 4 and assuming negligible direct feeding to the 123.2-keV state (since this transition will add to the 122.5-keV γ ray intensity) as discussed above, the internal conversion coefficient of the

52.6-keV γ ray was determined to be between 2.4 and 6.0. The large range is due to assuming all combinations of multipolarities for the 100.4-, 101.9-, 155.1-, and 122.5-keV γ rays (limited to $E1$, $M1$, and $E2$ from lifetime considerations, since all were seen to be in coincidence with other γ rays within the 30 nsec FWHM timing resolution of the experiment). The effects of the 100.4-, 101.9-, and 155.1-keV transitions are important because the intensities used to determine the 52.6-keV internal conversion coefficient were taken above the threshold for these transitions (to obtain good statistics). Since the theoretical conversion coefficients for a 52.6-keV transition are 1.06, 3.36, and 15.5 for $E1$, $M1$, and $E2$ multipolarities, respectively,¹⁴ an $M1$ assignment is strongly favored. Lastly, in light of the above analysis, if a multipolarity of $M1$ is assumed for the 52.6-keV transition, an $M1$ or $E1$ assignment is strongly favored for the 122.5-keV γ ray. The contributions from the other transitions mentioned were too small for multipolarity information to be obtained for them.

D. Spin assignments for ^{106}In from Hauser-Feshbach calculations

The Hauser-Feshbach theory¹⁵ was used to calculate the dependence on spin of the population of final states in the $^{106}\text{Cd}(p,n\gamma)^{106}\text{In}$ reaction. The applicability of this theory depends on a few key assumptions, namely that a statistical distribution of compound nucleus (CN) levels be available and that the incident beam energy resolution be broad enough to excite many of these levels. For protons incident on ^{106}Cd near the (p,n) threshold, the CN is at ~ 11 MeV in excitation. The level density here should be great enough; a simple Fermi gas model¹⁶ predicts $\omega(E) \sim 10^3/\text{keV}$. However, the presence of the ^{107}Cd ground state analog resonance and associated excited states, which lie in ^{107}In at ~ 9 MeV in excitation,¹⁷ could possibly distort the statistical distribution of reaction strength. On the other hand, the lack of gross fluctuations in the experimental excitation functions indicates that the level density is sufficiently high to permit the stochastic assumption discussed above. The spin dependence of the cross section then arises from spin-statistical factors for the CN states and the final state which, when coupled with the l dependence of the transmission coefficients, results in a strong dependence of calculated cross section on final-state spin.

Previous workers¹⁸ have inferred spins for states excited in $(p,n\gamma)$ reactions by comparing experimental cross sections to the calculations at bombarding energies several MeV above threshold. Here the γ cascade in the final nucleus to the state of interest is important. In the present experiment excitation functions for the various states were measured in small energy steps up to ~ 0.2 MeV above the threshold of each state. In this case, only the formation and decay of the CN is important. The situation is further simplified by the $J^\pi=0^+$ nature of the ^{106}Cd target.

The transmission coefficients for the calculations were obtained from the optical model code PTOLEMY.¹⁹ The

proton parameters were taken from Becchetti and Greenlees²⁰ and the neutron parameters from recent measurements by Smith²¹ of ^{115}In . Both sets are displayed in Table V. The inelastic channel is included using ^{106}Cd excited states with known J^π . In addition, the calculations require as input the other available final states in ^{106}In which can compete for reaction strength with the state of interest. The spins of these competing states are unknown, but are determined from the calculations by a bootstrap method which will be described below. It should be noted that in all cases the calculated quantity is $\int_{E_{\text{thresh}}}^{E_p} \sigma(E) dE$, in order to compare directly with the thick target yields measured in the experiment.

Initially, calculations were performed ignoring competition from states in ^{106}In . These calculations showed that $J_f=1,2$ would be populated the strongest, with $J_f=0,3,4$ somewhat weaker, and higher spins weaker still. It was also found that for $J_f \leq 4$ the parity of the final state had little effect on the calculated excitation functions.

The calculated neutron transmission coefficients indicated that a significant fraction of the final state neutrons emerge with $l=1$. This can be understood as a p -wave size resonance of the optical potential which is expected for $A \simeq 100$.²² These p -wave neutrons can cause the integrated yields to rise faster than $E_p^{3/2}$, such that $(\text{yield})^{2/3}$ vs E_p may no longer be linear. Detailed comparisons of the theoretical shapes of the curves with the measured 122.5-keV γ -ray excitation function showed that the extracted thresholds could differ by 5–8 keV from that determined from the $(\text{yield})^{2/3}$ method. As mentioned in Sec. IIIB a systematic error in the $^{106,108}\text{In}$ masses has been included for this effect but no correction has been made because the magnitude of the correction is completely model dependent.

The bootstrap method used in the comparison of theoretical and experimental excitation functions involves determining the best-fit spin for each state in ascending order of excitation. Once the spin of a state is determined its competition with the next higher-lying state is included. In order to compare the relative excitation functions, the spins of some states must be known. The spins of the ground state and β^+ -decaying isomer are known to be 7^+ (Ref. 11) and 3^+ (Ref. 23), respectively. In addition, experiments on the ^{106}Sn ($J^\pi=0^+$) β^+ decay have determined the 893.1- and 1219-keV states in ^{106}In to be 1^+ . The absence of direct β^+ feeding to other states⁵ (except for a possible weak feeding to the 151.1-keV level) indi-

cates there are no other low-lying $J=0,1$ states in ^{106}In .

As discussed above, the 122.5-keV γ ray from the decay of the 151.1-keV state (with negligible contribution from the 123.2-keV state) has the lowest threshold of the γ rays observed as well as the steepest excitation function. This suggests that its spin may be $J=1$ or 2. Because of the lack of strong β^+ feeding to this state in the ^{106}Sn decay,⁵ a spin of $J=1$ is not favored. Accordingly, a spin of $J=2$ was used in Hauser-Feshbach analysis of the excitation functions. However, due to the near equality of the slopes for the calculated $J=1$ and 2 excitation functions, the inferred spins for the higher-lying states are not sensitive to this assumption.

The relative integrated cross sections were determined from the experimental yields by correcting the yields for detector efficiency, branching ratio (from Refs. 1 and 5), and internal conversion. An $M1$ conversion coefficient was assumed in all cases, but it is significant only for $E_\gamma < 200$ keV. In fact, as discussed in Sec. IIIB, an $M1$ multipolarity is favored for most of the low-energy γ rays. In addition, the yields have been corrected for feeding from higher-lying states where appropriate. The overall cross section scale was set by normalizing the calculation for the 122.5-keV γ ray to the measured excitation function. Calculations were performed for a range of final-state spins. Comparisons of the calculations and measurements are shown in Fig. 5. In some cases excitation functions were calculated assuming a negative parity for the state, to show the lack of sensitivity of the calculations to the parity of the state. Spins for the various states inferred from the above analysis are shown in Fig. 4 with the preferred spins listed first.

The 386.8-keV excitation function in Fig. 5(g) appears to be somewhat below the predictions for a $J=1$ spin assignment for the 893.1 keV state (inferred from previous ^{106}Sn β^+ decay work⁵), although not substantially. This could be partly due to an incorrect spin assignment to several of the lower-lying states or to some unknown low spin states not placed in the level scheme. Also plotted as a dashed line in Fig. 5(g) is the predicted 1^+ excitation function for the 386.8-keV γ ray if the 151.1-keV level is assumed to be $J=3$ rather than $J=1$ or 2. This is clearly inconsistent with the measurements.

E. Mass of $^{108}\text{In}(3^+)$

The laboratory thresholds of the 168- and 236-keV γ rays produced via $^{108}\text{Cd}(p,n\gamma)^{108}\text{In}$ were used to determine

TABLE V. Optical-model parameters used to calculate the transmission coefficients.

V (MeV)	V'	W_s (MeV)	r_0 (fm)	a (fm)	r_s (fm)	a_s (fm)
Protons						
60.0	-0.32	12.7	1.17	0.75	1.32	0.56
Neutrons						
49.9	-0.30	5.82	1.23	0.68	1.27	0.52

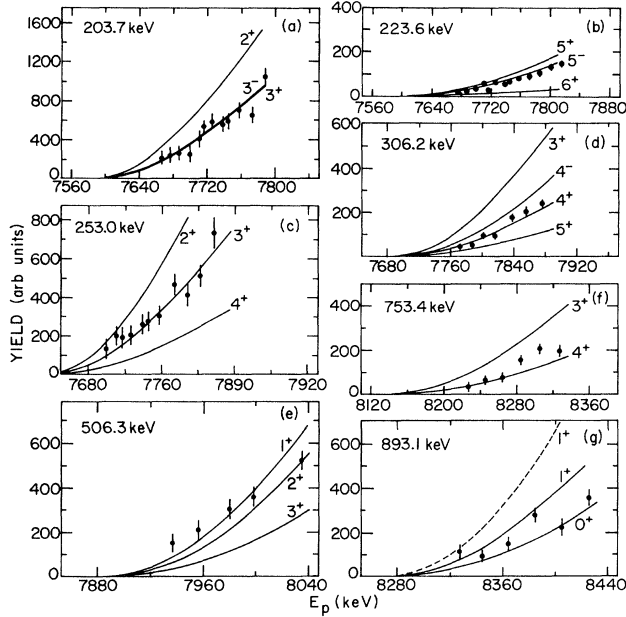


FIG. 5. Relative γ -ray excitation functions corrected for detector efficiency, branching ratio, and internal conversion. The solid lines are the statistical-model calculations for the various spins.

the mass excess of the $J^\pi = 3^+ \beta^+$ -decaying state of ^{108}In . Based on the level scheme of Hseuh and Macias¹² deduced from in-beam and β^+ -decay work, these γ rays decay directly to $^{108}\text{In}(3^+)$ and therefore have a relative separation of 68 keV. The measured thresholds in the present experiment for the 168- and 236-keV transitions were 6191 ± 8 keV and 6244 ± 9 keV, respectively, with an energy difference of 53 ± 12 keV which is consistent with the above separation. Feeding from higher-lying states was estimated to be negligible from the transition intensities of Ref. 12. The above two γ -ray thresholds give an $^{108}\text{In}(3^+)$ mass excess of -84018 ± 12 keV where the error results from effects discussed in Sec. III D. This new value for the mass excess is in agreement with the previous value of -84100 ± 80 keV,² but the uncertainty has been greatly reduced. The uncertainty in the mass excess of ^{108}Sn is also improved; when the inferred Q_{ec} value of Ref. 1 is combined with the present work a mass excess of -81970 ± 30 keV is obtained for ^{108}Sn .

IV. DISCUSSION

The low-lying levels in the odd-odd In isotopes with $A = 106-110$ are shown in Fig. 6. The present work has established the energy separation of the high-spin ground state and low-spin isomer in ^{106}In to be 28.6 ± 0.5 keV. The separation of low-lying levels for $^{108,110}\text{In}$ is unknown, although there is some indication from β^+ -decay work²⁴ that the separation for ^{108}In is small (40 ± 70 keV), with the high-spin state lower in energy. The isomerism and perhaps even the low-lying spins can be understood in terms of the j - j coupling model and the coupling rules of Brennan and Bernstein.²⁵ In the j - j coupling model the

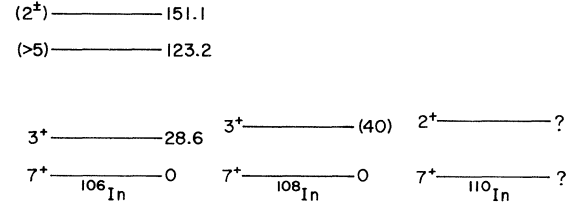


FIG. 6. Low-lying levels in $^{106,108,110}\text{In}$.

neutron-proton residual interaction is assumed to be much weaker than the spin-orbit force. The low-lying levels in odd-odd nuclei are then determined by the coupling of the odd neutron and proton single-particle states into a single configuration. Which single-particle states are important is determined from the adjacent odd-proton and odd-neutron nuclei. As the residual interaction is turned on, the various spins resulting from the single neutron-proton configuration are split into $J_p + J_n - |J_p - J_n|$ different levels. The Brennan and Bernstein rules then predict which of these spins will be low-lying states in the nucleus.

The odd- A In nuclei near $^{106,108}\text{In}$ indicate unambiguously a ground-state proton configuration of $(\pi g_{9/2})^{-1}$, with the $(\pi p_{1/2})^{-1}$ state lying $\sim 600-700$ keV higher. The adjacent odd-neutron Cd nuclei all have ground-state spins of $\frac{5}{2}^+$, indicating the presence of an unpaired neutron in the $d_{5/2}$ shell. If this is assumed to be a single neutron hole state, then the Brennan and Bernstein rule R2 predicts low-lying states of $J = |J_1 \pm J_2| = 2^+$ and 7^+ . Indeed, Fig. 6 shows that $^{106-110}\text{In}$, with low-lying $J = 7$ states, are in accordance with this prediction. In addition, a low-lying $J = 2$ state is likely to be present in all three nuclei but is an isomer only in ^{110}In . For $^{106,108}\text{In}$ the first excited state is a 3^+ isomer, signaling perhaps the presence of the $(\nu g_{7/2})^{-1}$ configuration. In fact, the magnetic-moment measurements of Vandeplasche *et al.*¹¹ indicate that for $^{108}\text{In}(3^+)$ the dominant configuration is $[(\pi g_{9/2})^{-1}(\nu g_{7/2})^{-1}]_{3^+}$. These same experiments also show a significant contribution from the $[(\pi g_{9/2})^{-1}(\nu d_{5/2})^{-1}]_{7^+}$ configuration for $^{106,108}\text{In}(7^+)$, in agreement with the discussion above.

It is clear that a detailed discussion of the trends and the breakdown of trends in the even- A In isotopes awaits further experimental information. In particular, definite spin and parity assignments and the relative locations of the ground states and isomers would be useful.

ACKNOWLEDGMENTS

The authors would like to acknowledge helpful discussions with J. P. Schiffer and P. A. Moldauer. We also wish to thank J. L. Yntema and the tandem staff for assistance with the experiment. This work was supported by the U. S. Department of Energy under Contract W-31-109-Eng-38.

- *Present address: W. K. Kellogg Radiation Laboratory, California Institute of Technology, Pasadena, CA 91125.
- ¹A. Plochocki, G. M. Gowdy, R. Kirchner, O. Klepper, W. Reisdorf, E. Roeckl, P. Tidemand-Petersson, J. Zylicz, U. J. Schrewe, R. Kantas, R.-D. von Dincklage, and W. D. Schmidt-Ott, Nucl. Phys. **A232**, 29 (1979).
 - ²A. H. Wapstra and K. Bos, At. Data Nucl. Data Tables **19**, 175 (1977).
 - ³R. C. Catura and J. R. Richardson, Phys. Rev. **126**, 646 (1962); Nucl. Phys. **82**, 471 (1966).
 - ⁴V. N. Burminskii, I. V. Grebenshchikov, O. D. Kovrigin, and G. I. Sychikov, JETP Lett. **22**, 54 (1975).
 - ⁵B. J. Varley, G. S. Foote, C. Garrett, and W. Gelletly, J. Phys. G **4**, 1643 (1978).
 - ⁶C. L. Starke, E. A. Phillips, and E. H. Spejewski, Nucl. Phys. **A139**, 33 (1969).
 - ⁷V. Metag, R. Repnow, and J. L. Durell, Phys. Lett. **38B**, 19 (1972).
 - ⁸S. Flanagan, R. Chapman, J. L. Durell, W. Gelletly, and J. N. Mo, J. Phys. G **2**, 589 (1976).
 - ⁹H. Huang, B. P. Pathak, and J. K. P. Lee, Can. J. Phys. **56**, 936 (1978).
 - ¹⁰I. N. Wischniewski, H. V. Klapdor, P. Herges, H. Fromm, and W. A. Zheldonozhski, Z. Phys. A **298**, 21 (1980).
 - ¹¹D. Vandeplasseche, E. van Walle, C. Nuytten, and L. Vanneste, Phys. Rev. Lett. **49**, 1390 (1982).
 - ¹²H.-C. Hseuh and E. S. Macias, Phys. Rev. C **17**, 272 (1978).
 - ¹³J. M. Freeman, Nucl. Instrum. Methods **134**, 153 (1976).
 - ¹⁴F. Rösel, H. M. Fries, K. Alder, and H. C. Pauli, At. Data Nucl. Data Tables **21**, 91 (1978).
 - ¹⁵W. Hauser and H. Feshbach, Phys. Rev. **87**, 366 (1952).
 - ¹⁶A. Bohr and B. Mottelson, *Nuclear Structure* (Benjamin, New York, 1969), Vol. 1.
 - ¹⁷E. Abramson, I. Plessner, and Z. Vager, Phys. Lett. **26B**, 723 (1968).
 - ¹⁸See, for example, L. E. Samuelson, W. H. Kelly, R. R. Todd, R. A. Warner, Wm. C. McHarris, F. M. Bernthal, E. M. Bernstein, and R. Shamu, Phys. Rev. C **7**, 2379 (1973); K. Ashibe and H. Taketani, Nucl. Phys. **A255**, 360 (1975); W. Dietrich and A. Bäcklin, Z. Phys. A **276**, 133 (1976); M. Adachi, A. Muroi, T. Matsuzaki, and H. Taketani, *ibid.* **295**, 251 (1980).
 - ¹⁹M. H. Macfarlane and S. C. Pieper, Argonne National Laboratory Report ANL-76-11 Rev. 1, 1976 (unpublished).
 - ²⁰F. D. Becchetti and G. W. Greenlees, Phys. Rev. **182**, 1190 (1969).
 - ²¹A. B. Smith (private communication to P. A. Moldauer).
 - ²²E. Vogt, in *Advances in Nuclear Physics*, edited by M. Baranger and E. Vogt (Plenum, New York, 1968), Vol. 1.
 - ²³B. Harmatz, Nucl. Data Sheets **30**, 305 (1980).
 - ²⁴T. Katoh, M. Nozawa, and Y. Yoshizawa, Nucl. Phys. **36**, 394 (1962).
 - ²⁵M. H. Brennan and A. M. Bernstein, Phys. Rev. **120**, 927 (1960).